Toughness Improvement of Epoxy Networks by Nanophase-Separating Antiplasticizers

L. Laiarinandrasana,[1] Y. Fu,[2] J. L. Halary[2]

[1]*MINES ParisTech, Centre des Matériaux - CNRS UMR 7633, BP 87, 91003 Evry Cedex (France)*
[2]*ESPCI ParisTech, SIMM Lab. - CNRS UMR 7615, 10 rue Vauquelin, 75231 Paris Cedex 05 (France)*

Received 18 February 2011; accepted 7 April 2011
DOI 10.1002/app.34646
Published online 15 September 2011 in Wiley Online Library (wileyonlinelibrary.com).

ABSTRACT: Two epoxy-amine networks were toughened by using a nanophase separating antiplasticizer at various contents ranging from 0 to 20 mol % with respect to the epoxide. These model networks were chosen to differ markedly by their glass transition temperature in the absence of additive, namely 180°C and 114°C. Net stress was measured as a function of crack opening displacement on single edge notch bending specimens. Analysis of the experimental data yielded both stiffness and fracture toughness. In addition, fracture surfaces were observed by scanning electron microscopy. Effect on both stiffness and toughness of network characteristics (nature of the hardener, amount of additive) were carefully examined. Conditions were found for which fracture energy at crack initiation substantially increases without any detrimental effect on stiffness. © 2011 Wiley Periodicals, Inc. J Appl Polym Sci 123: 3437–3447, 2012

Key words: epoxy-amine network; fracture mechanics; toughening; antiplasticizer; nanophase separation

INTRODUCTION

Structural polymers are more and more used in engineering components submitted to thermomechanical loadings. Mechanical behavior and fracture characteristics are key factors to assess the durability of such components. To this end, toughness of polymeric materials is often characterized by the impact strength (from Charpy or Izod tests). These are dynamic tests carried out at high strain rate level or equivalently at temperatures well below their glass transition temperature, T_g (glassy polymers). Indeed, if the test temperature is near or above T_g, then impact strength would be inappropriate to determine the failure behavior of the material. Fracture mechanics approaches give an accurate definition of fracture toughness. For materials presenting a linear elastic response, the values at failure of the stress intensity factor or of the energy release rate are considered to be the relevant parameters. Comprehensive research has been carried out for years on metallic materials concerning the equivalence between impact strength and fracture toughness.[1–3] It turned out that this equivalence may be obtained in the low fracture energy domain that is in brittle fracture.

To the authors' knowledge, there is no such amount of work on polymers. Some attempts were made in this way but failed because, for instance, of the difficulty to fulfill requested plane strain conditions. Nevertheless, impact strength or toughness of polymeric materials are often plotted against various parameters including the test temperature (to find a ductile (high fracture energy) to brittle (low fracture energy) transition temperature) or the average ligament thickness (mean interdistance between toughening particles).[4] The essential motivation of such a plot is to check whether the modification of the material process actually leads to an improvement of the toughness or the impact strength.

This article focuses on the case of epoxy networks of industrial interest. These polymeric materials are basically brittle and need to be toughened by soft particles in the perspective of applications.[5] A classical route to the toughening of epoxy network is the incorporation of reactive diluents or the dispersion of core-shell particles within the rigid thermoset. Unfortunately, both strategies lead to a dramatic decrease of Young's modulus when toughening is successfully achieved.

Quite recently, an alternative approach of epoxy toughening has been reported, using soft inclusions of a new type that work over a broad range of epoxy-amine resins, including complex commercial formulations.[6] This approach is based on the use of antiplasticizers that are small molecules which behave as a modulus fortifier with respect to the polymer.[5,8] Further benefits can be expected using

Correspondence to: L. Laiarinandrasana (lucien.laiarinandrasana@mines-paristech.fr).

© 2011 Wiley Periodicals, Inc.

TABLE I
Chemical Formulae of the Sample Components

Acronym	Chemical formula
DGEBA	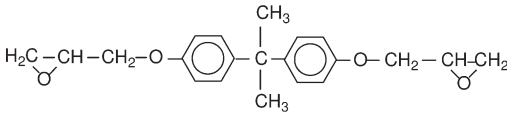
DDM	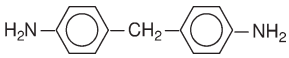
HMDA	$H_2N-(CH_2)_6-NH_2$
AP-additive	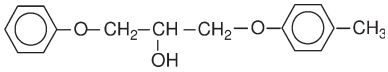

the pioneering ideas on chemically induced phase separation technique.[9] In our case, if the antiplasticizer is designed to be fully miscible to the mixture of monomers but to phase separate before gelation in the form of soft clusters of nanometric size, then toughening is observed without any loss of materials modulus.[6,7] However, some decrease of T_g cannot be avoided.

This article aims at providing a deeper understanding of the toughening mechanism of epoxy-amine resins by nanophase-separating antiplasticizers. To this end, some model formulations were used, consisting of the usual diglycidylether of bisphenol-A (DGEBA) as the epoxide and diaminodiphenylmethane (DDM) or hexamethylenediamine (HMDA) as the hardener. The antiplasticizer (AP) (1-tolyloxy, 3-phenoxy, propane-2 ol) shown in Table I was selected as the toughening agent among different candidates[7] because of its well documented behavior.

These materials are such that linear elastic fracture mechanics concepts can be applied when tests are carried out at room temperature. First, some details concerning the formulation of the materials of the study and the experimental setup used for fracture toughness measurement will be given. Then, the experimental results will be discussed by considering all the parameters that enable evaluation of the toughening effect. And finally, an attempt will be made to extract the relevant parameter with respect to which toughening effect is observed.

EXPERIMENTAL

Materials

Formulae of the chemicals used in this study are given in Table I. DGEBA, DDM, and HMDA are high-purity commercial chemicals, supplied by Bakelite for DGEBA (Rutapox 162) and by Sigma-Aldrich for the others. The antiplasticizer, a noncommercial chemical that will be named "AP-additive" in the following, is the product of reaction of phenylglycidylether and *p*-cresol. Synthesis conditions of AP have been detailed elsewhere.[6]

DGEBA and DDM/HMDA were used in stoichiometric proportions (one epoxide ring per one *N*-H amine function). In other words, the molar fraction of diepoxide was twice as large as that of diamine. The amount of AP-additive was adjusted at 0 mol %, 10 mol % and 20 mol % of the epoxide amount. The mixtures were cured at 80°C for 12 h and then postcured at 160°C for 24 additional hours. These cure conditions are those recommended by the manufacturer in the absence of our additive.

It is worth pointing out that no chemical reaction takes place between the additive and the network, as checked by infra-red and nuclear magnetic resonance spectroscopies.

About the nomenclature used throughout the article to designate the samples, DGEBA is not specified since it is systematically used. Therefore, each sample is simply named by the acronym of the hardener (DDM or HMDA) followed by the AP-additive content. For instance DDM10% stands for DGEBA/DDM/10 mol % AP-additive.

Dynamic mechanical analysis

Viscoelastic experiments were performed on a dynamic mechanical analyzer TA Instruments Q800, operated in the 3-point bending mode, at the frequency 1 Hz and over the temperature range −150°C/200°C. Values of the storage modulus, E' and loss modulus, E'', were calculated as the real and imaginary components of the complex modulus E^*. Inspection of peaks of E'' allows the identification of the mechanically active relaxations, whereas E' can be regarded as the Young's modulus of the material at the considered temperature.

Differential scanning calorimetry

Thermal analysis experiments were performed on a Differential Scanning Calorimeter Q200 (TA Instruments), operated at a heating rate of 10 K min^{-1} over the temperature range −150°C/200°C. Two successive runs were performed, and T_g was taken as the temperature where the onset of heat capacity is detected during the second run.

Toughness measurements

The determination of the toughness was performed on Single Edge Notch Bending (SENB) specimens machined from plates of 160 mm × 80 mm × 7 mm,

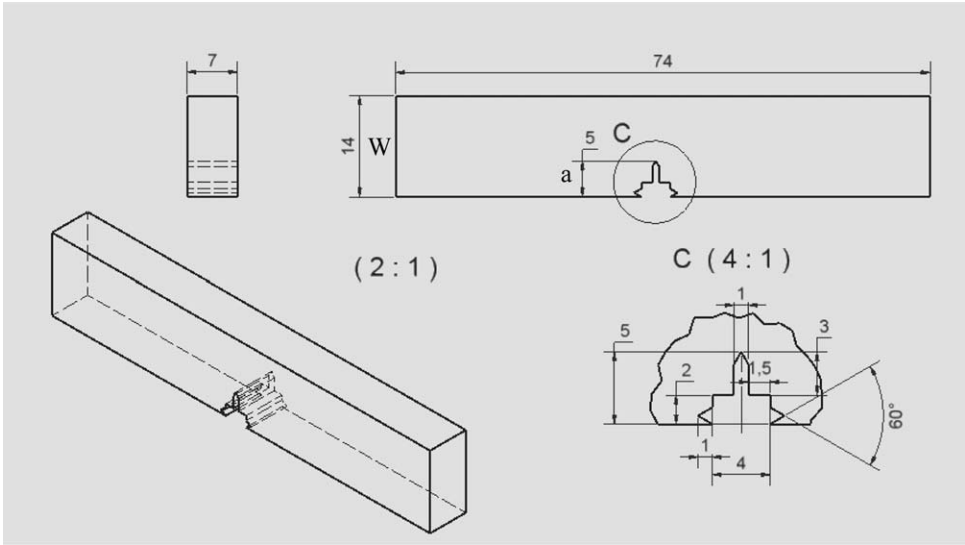

Figure 1 Sketch of the SENB specimen. Characteristic dimensions are crack depth $a = 5$ mm; specimen width $W = 14$ mm; thickness $t = 7$ mm, uncracked ligament (W-a) = 9 mm.

manufactured at ESPCI ParisTech. Figure 1 sketches a SENB specimen. The precrack was also machined with a notch radius of $\sim$ 100 μm. Machining the crack allowed a better control of the geometry of all specimens. Accordingly, the crack depth is fixed at $a = 5$ mm over a width of $W = 14$ mm, giving a fixed crack depth ratio of $a/W = 0.36$. The thickness is equal to $t = 7$ mm.

Before investigating various characteristic parameters at crack initiation, fracture surfaces were examined with the help of Scanning Electron Microscope (SEM). Prior to microscopic observations, Au-Pd coating was applied to the fracture surfaces.

The experimental setup is shown in Figure 2. An Inströn testing machine was used at a constant crosshead speed of 0.5 mm s^{-1}. SENB specimens were tested using a span to specimen width ratio S/W of 40 : 14. Deflection and load were monitored together with the crack opening displacement (COD) measured using a MTS extensometer. COD will be referred to as δ in the following. For the sake of reproducibility, all tests were repeated three times.

RESULTS AND DISCUSSION

Antiplasticization and phase separation

Let us consider, as a selected example, the DGEBA-DDM network. Inspection of the DMA traces of DGEBA-DDM, either neat or in the presence of the 20% additive AP (Fig. 3), gives evidence for some essential features. The E'' plot relative to neat DGEBA-DDM shows two mechanically active relaxations,[6] namely the α relaxation at high temperature, in the glass transition region, and the β relaxation, at lower temperature, that mainly involves hydroxypropylether motions. With DDM20%, presence of the additive AP is marked by plasticization effects in the glass transition region (substantial decrease of T_α down to 110°C), and by antiplasticization effects in the secondary relaxation region (dramatic reduction of the E'' peak). In addition, the modified sample

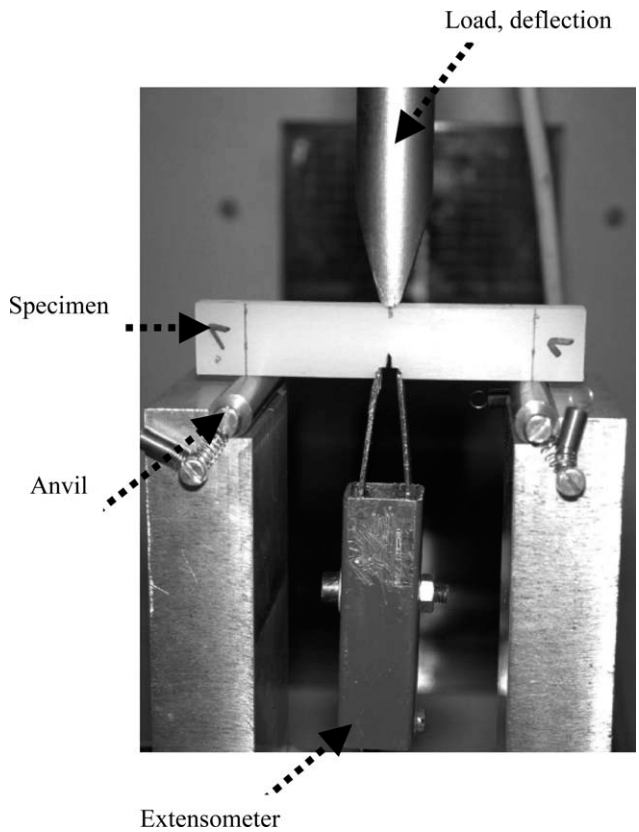

Figure 2 Experimental setup, extensometer equipment for opening displacement measurement. The span (distance between anvils) is $S = 40$ mm.

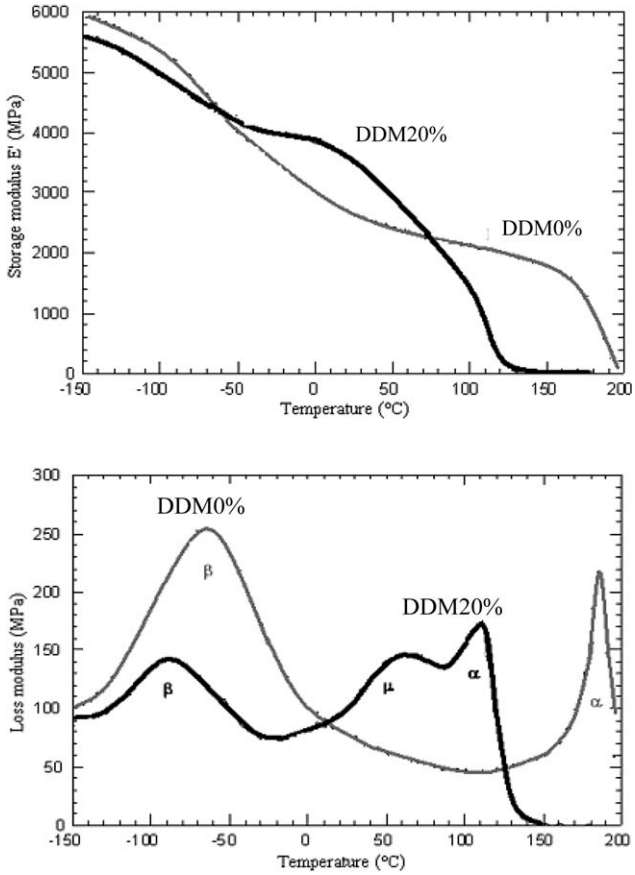

Figure 3 Influence of the AP-additive on the DMA traces of DGEBA-DDM (after[6]).

presents a splitting of the high temperature relaxation into two peaks, so-called α and μ. As far as the E' traces are concerned, the antiplasticizing effect of the additive AP shows up. In each case, an increase in E' is observed upon addition of additive at temperatures ranging from T_β to T_α.

The next question refers to the origin of the μ relaxation. As sketched in Figure 4, the additive AP is miscible to the initial mixture of DGEBA and DDM but gives rise to nano-scale phase separation during the network construction step. This phenomenon relates the occurrence of phase separation to changes in the phase diagram when the polymer chain length increases. Evidence for this phenomenon cannot be given by Transimission Electron Microscopy because of the lack of contrast between the two phases. However, occurrence of the phase separation has been provided by solid-state ^{1}H NMR measurements.[10]

A crude calculation of the additive abundance in phases α and μ can be made knowing the values of T_α and T_μ and the glass transition temperature of the additive.[6] It turns out that the domains occupied by the phase α are strongly predominant in the materials (about 85%) and that they consist of polymer segments in interaction with a restricted number of additive molecules. The other additive molecules, which are rejected out of the phase α during the network formation, are also of a minority (about 40%) in the phase μ. This very special morphology has a strong influence on the resin toughness.[5] Figure 5 clearly shows that the critical energy release rate (G_{IC}) was increased, especially at high test temperature, upon addition of 20mol% of AP-additive.

The qualitative DMA behavior of DDM20% remains the same for DDM10% and HMDA10%. However, from a quantitative point of view, the effect of AP is less marked in terms of T_α decrease, antiplasticizing effect, μ-phase extent and, in turn, increase of G_{IC}. The situation of HMDA20% is more confusing with regard to the μ phase observation. Indeed, the T_α decrease is sufficiently large in this case so that the glass transition temperatures of the α and μ phases are likely to merge. Although the data are not shown here for the sake of concision, the antiplasticizing effect of AP on the β peak is observed, almost with the same importance as for DDM20%.

Glass transition temperature of the α phase

The effect of AP additive content on the T_g of the a phase was checked by DSC. Table II summarizes these values together with some characteristic temperature gaps that will be used later on in the article. Two important points have to be made: (1) The T_g

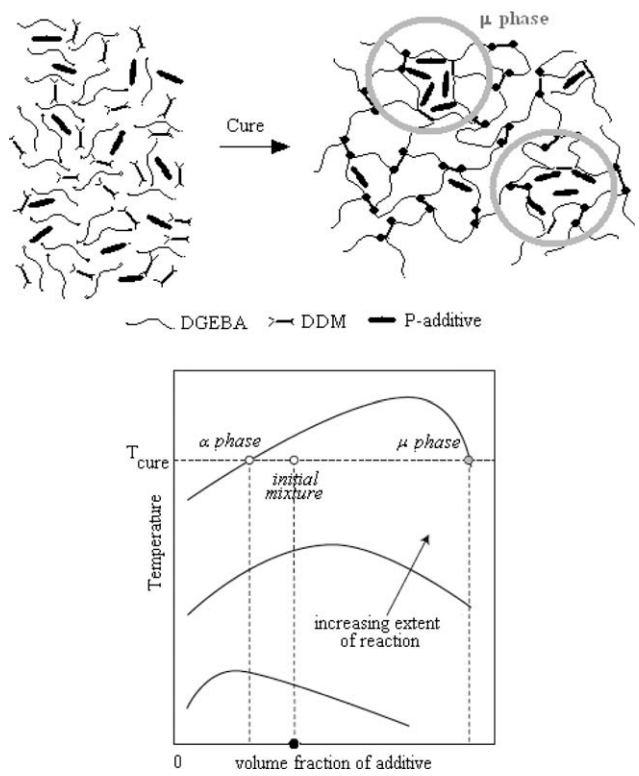

Figure 4 Scheme of the μ-phase formation in the presence of additive (after[6]).

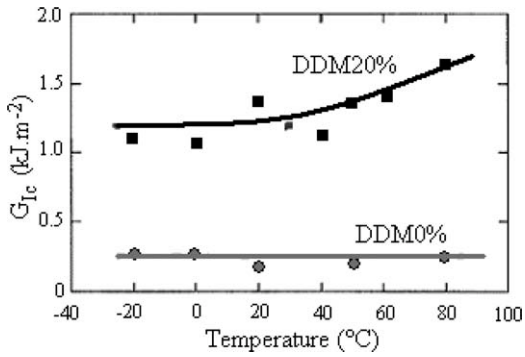

Figure 5 Toughening effect due to 20 mol % AP-additive on DGEBA-DDM system (after[6]).

(DSC) values are in quite good agreement with the T_α (DMA) values; and (2) the DSC traces do not reveal the existence of the T_g of the μ phase, probably as the result of a lack of sensitivity of the technique.

Curves of net stress versus δ

Following fracture mechanics concepts, the key curves concern the evolution of the net stress as a function of the crack opening displacement δ. The net stress was calculated as the measured load divided by the net section (7 mm × 9 mm). For the sake of clarity, a unique curve shows up in Figure 6 for each material: however, each curve is the result of the average values on three separate experiments. Plots in Figure 6 were set at the same scale to compare some characteristic parameters. The shape of these curves is classical for SENB tests. Two stages can be distinguished:

- the loading stage (up to maximum net stress), considered as under stationary crack corresponding to the initial value of $a/W = 0.36$. This part is concerned with "crack initiation" process;
- and the crack growth stage, characterized by the decrease of net stress. Although the crack growth rates are high, some experimental points during this stage were recorded. These data could be utilized to analyze the rapid crack propagation but this objective is out of the scope of the present article.

TABLE II
Evolution of Glass Transition Temperature (DSC) with Respect to AP Additive Contents

DGEBA	AP (%)	T_g (°C)	T_g (0%) − T_g (K)	$T_{test} - T_g$ (K)*
	0	180	0	−160
DDM	10	127	53	−107
	20	95	85	−75
	0	114	0	−94
HMDA	10	78	36	−58
	20	55	59	−35

** $T_{test} = 20°C$

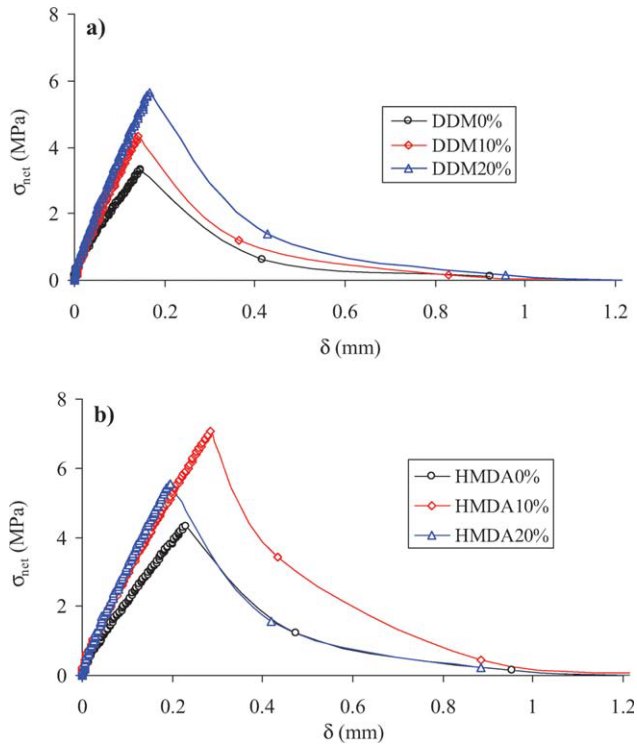

Figure 6 Net stress versus crack opening displacement curves: (a) DDM; (b) HMDA. [Color figure can be viewed in the online issue, which is available at wileyonlinelibrary.com.]

For DDM material [Fig. 6(a)], stiffness is quite similar for DDM10% and DDM20%. In addition, it can be observed that the higher the AP-additive content, the higher the maximum net stress. Conversely, in Figure 6(b), the stiffness seems also to be approximately the same for HMDA10% and HMDA20% but the maximum net stress of HMDA20% seems to be abnormally low as compared with HMDA10%.

To have an insight in the crack initiation stage, attention is focused only the loading part of the net stress versus δ (Fig. 7). It should be mentioned that that the reproducibility is well established. It can be observed that all curves in Figure 7 are quasi-linear. The above-mentioned comparison between maximum stresses is confirmed. Arrows indicate the maximum stress levels for each material. Additionally, Figure 7(b) clearly shows that the stiffness of HMDA10% and HMDA20% is the same.

Linear plot of net stress versus δ partially validates the use of linear elastic fracture mechanics (LEFM).

Fractography

Figure 8 shows fractography of DDM materials. Generally, brittle fracture surfaces were observed. The initiation sites were located near to the crack front they are indicated by white arrows in the left hand figures. Right hand pictures illustrate pattern

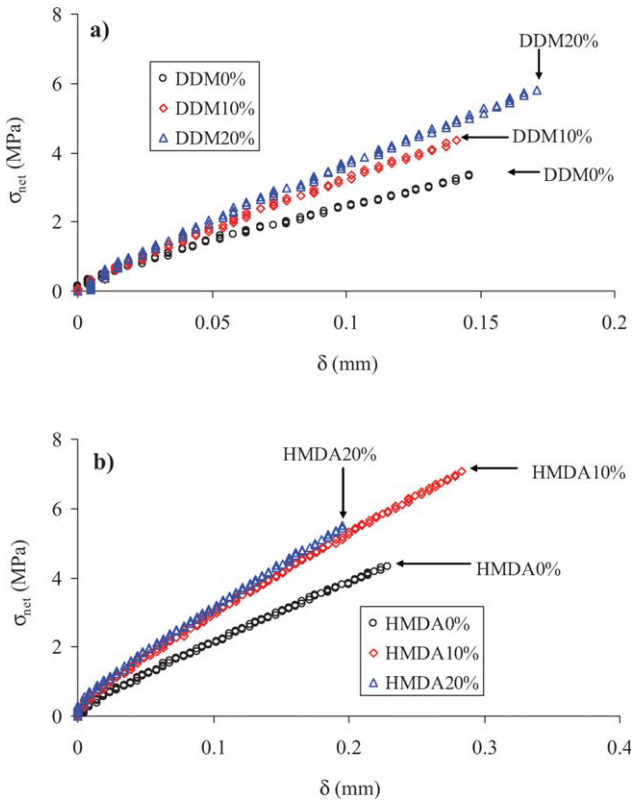

Figure 7 Net stress versus crack opening displacement curves up to maximum net stress (crack initiation) (a) DDM; (b) HMDA. [Color figure can be viewed in the online issue, which is available at wileyonlinelibrary.com.]

showing "leaves" printed by the crack propagation. The arrows indicate the direction of propagation. The width of these leaves increases with the AP-additive content. No dimple was observed and micro-shearing seems to appear at the boundary of each leave. The propagation part will not be considered further, however all of the observations confirmed that the fracture has occurred in a brittle way. This validates once again the use of LEFM concepts.

HMDA materials fractography in Figure 9 shows smoother fracture surfaces. Leaves are less visible. The "white particles" seen on the examined surfaces may be disregarded: they presumably result from some carbonatation of HMDA during monomer mixing. Salient features were observed for HMDA 20% material: the fracture surfaces are completely flat, without any pattern (leaves) but other unexpected objects could be found. For instance, in Figure 9(c) (right), black points seem to be voids whereas unidentified white objects appear all over the observed surface. The observations indicate that this material has peculiar properties as regard to the five others.

Characteristic parameters at crack initiation

In this section, all characteristic parameters corresponding to the maximum net stress—that is at crack initiation—are analyzed with respect to the

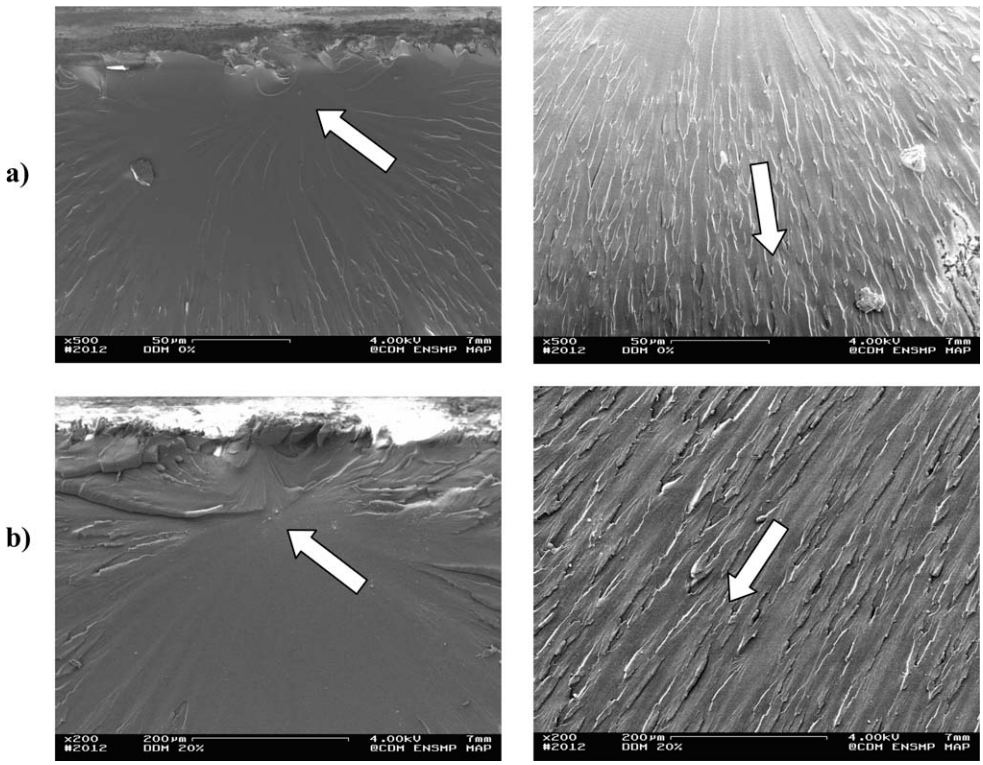

Figure 8 Fractography for DDM material (a) 0% AP additive; (b) 20% AP additive.

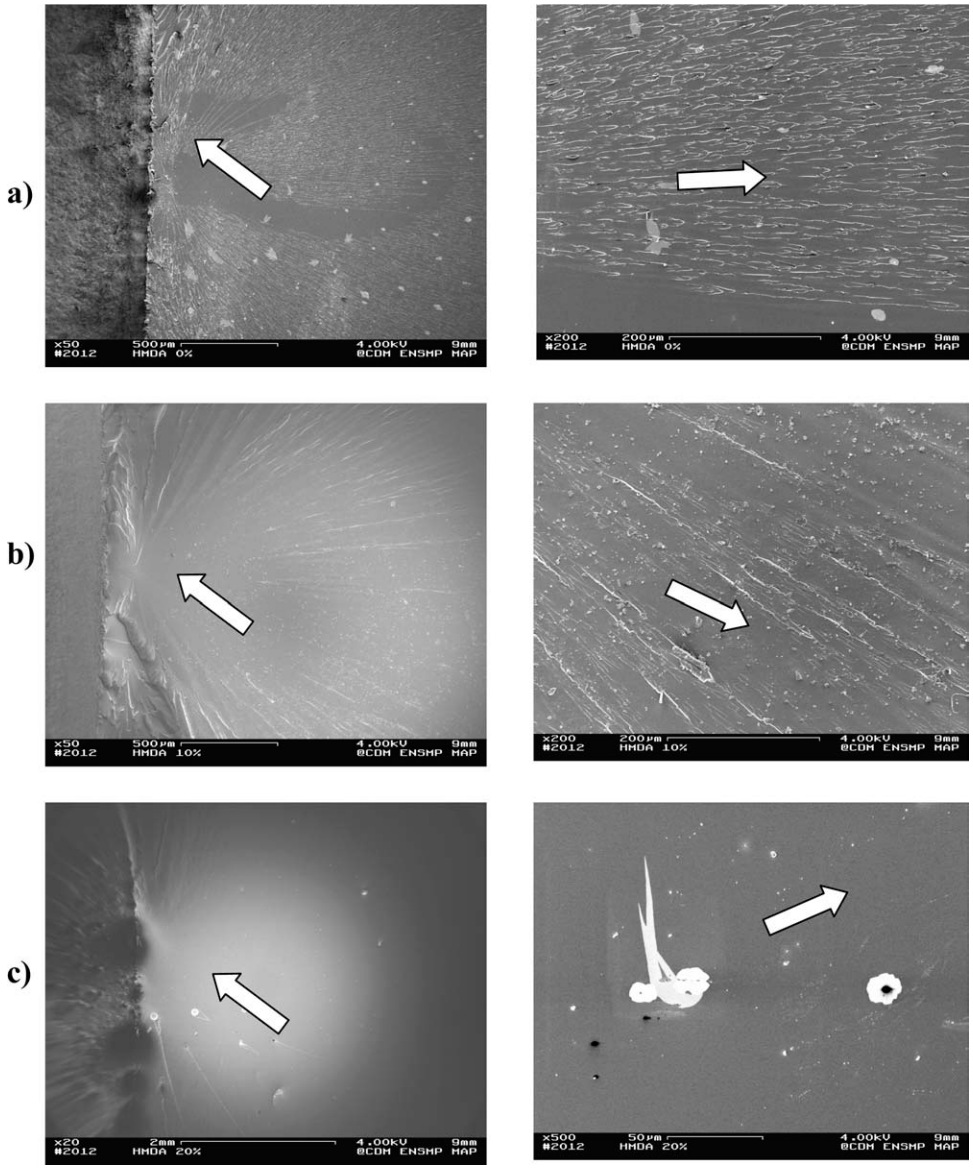

Figure 9 Fractography for HMDA materials (a) 0% AP additive; (b) 10% AP additive; (c) 20% AP additive.

AP-additive contents. The goal is here to exclusively use experimental data issued from the fracture tests. To this end, the Young's modulus and the toughness will be related to experimental characteristics such as the stiffness and the area under net stress versus δ, respectively. The loading curve, up to the maximum net stress, will then be utilized to investigate the toughness improvement.

Maximum net stress

Figure 10a shows the evolution of the maximum net stress when the AP-additive percentage is increased for both materials. For unfilled resin networks, the decrease in T_g (from 180°C for DDM0% to 114°C for HMDA0%) resulted in an unexpected slight increase of the maximum net stress. Moreover, HMDA material exhibits greater increase in the maximum net stress than DDM material for the same increase of 10% AP-additive content. Note that for DDM material this gain is about 1MPa compared with 2.5 MPa for HMDA material. Whereas the increase in maximum net stress is observed for DDM material from 10 to 20% AP-additive contents, HMDA shows a decrease, as it was already mentioned. The maximum stresses of DDM20% and HMDA20% are at quite similar value but in the authors' opinion, it is completely fortuitous.

δ at maximum net stress

The same analysis as for maximum net stress is carried out for the δ at initiation, i.e., corresponding to the maximum net stress [Fig. 10(b)]. First, for

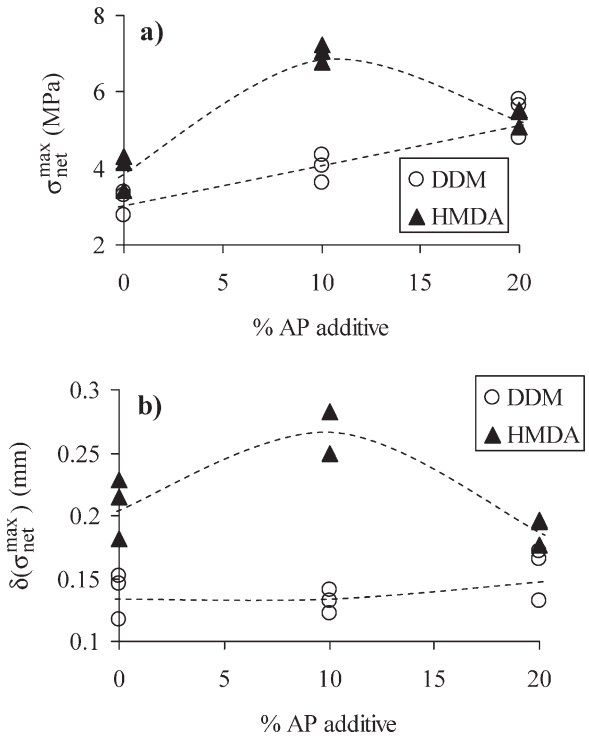

Figure 10 Characteristic parameters plotted against AP-additive content for DDM and HMDA materials: (a) Maximum net stress; (b) δ at maximum net stress. Dashed lines were drawn to highlight the observed trends.

unfilled resins, HMDA shows higher value of δ than that of DDM. δ being related to the ductility of the material, it seems then that decreasing T_g resulted in increasing the ductility without diminishing the maximum stress reached by the material. From 0 to 10% AP-additive, DDM shows lower increase in the critical δ than that of HMDA. This latter observes once again a decrease of the δ at initiation when increasing the AP-additive content from 10 to 20%.

Stiffness versus Young's modulus

According to Tada et al.,[11] the opening displacement for a SENB specimen, function of the net stress, is given by the following formula:

$$\delta(\sigma_{net}) = 6\frac{S\sigma_{net}}{E'}\left(1-\frac{a}{W}\right)\frac{a}{W}V_1\left(\frac{a}{W}\right), \quad (1)$$

with

$$V_1\left(\frac{a}{W}\right) = 0.76 - 2.28\left(\frac{a}{W}\right) + 3.87\left(\frac{a}{W}\right)^2 - 2.04\left(\frac{a}{W}\right)^3 + \frac{0.66}{\left(1-\frac{a}{W}\right)^2}. \quad (2)$$

In these expressions, S is the span, E' is the Young's modulus E in plane stress and $E/(1-\nu^2)$ in plane strain conditions, respectively, with ν the Poisson's ratio.

From eq. (1), one can deduce the stiffness (reverse of the compliance) as follows:

$$\frac{\sigma_{net}}{\delta(\sigma_{net})} = \frac{E'}{6S\left(1-\frac{a}{W}\right)\frac{a}{W}V_1\left(\frac{a}{W}\right)}, \quad (3)$$

where it can be observed that apart from E' the right hand term is exclusively geometrical. Since the characteristic dimensions of the specimens are the same for all materials, the stiffness evolution deals with that of the Young's modulus. Additionally, the net stress versus δ curve being linear, the stiffness was calculated for each test as $(\sigma_{net}^{max}/\delta(\sigma_{net}^{max}))$. This definition allows highlighting the evolution of the Young's modulus according to the AP-additive content. Figure 11 illustrates this evolution: by increasing the AP-additive content, the stiffness continuously increases for both resins. As mentioned in section Antiplasticization and phase separation, the addition of antiplasticizer leads to improvement of Young's modulus. However, for HMDA, the increase in Young's modulus between 10 and 20% antiplasticizers is smaller than for DDM. The graph seems to indicate that a plateau is likely to be reached. For unfilled resins, it was mentioned that σ_{net}^{max} is approximately the same whereas corresponding $\delta(\sigma_{net}^{max})$ is higher for HMDA0% than that of DDM0%. It turns out that the stiffness of HMDA0% is lower than that of DDM0%. Moreover, the increase in stiffness related to that of the AP-additive content is approximately the same for both resins. This conclusion is consistent with the observations reported in section Antiplasticization and phase separation.

Fracture energy at crack initiation versus toughness

One of the major difficulties to compare the toughness for brittle and ductile materials is the choice of the relevant parameter. In this article, the more

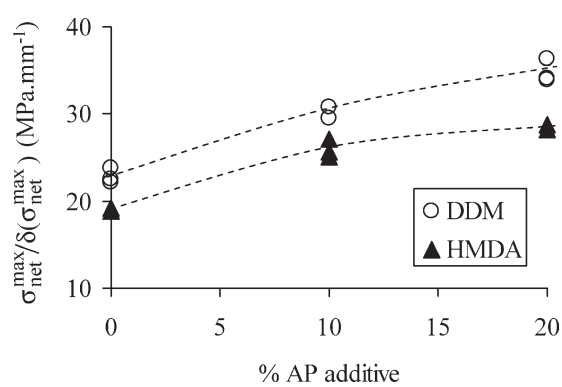

Figure 11 Stiffness plotted against AP-additive content for DDM and HMDA materials. Dashed lines were drawn to highlight the observed trends.

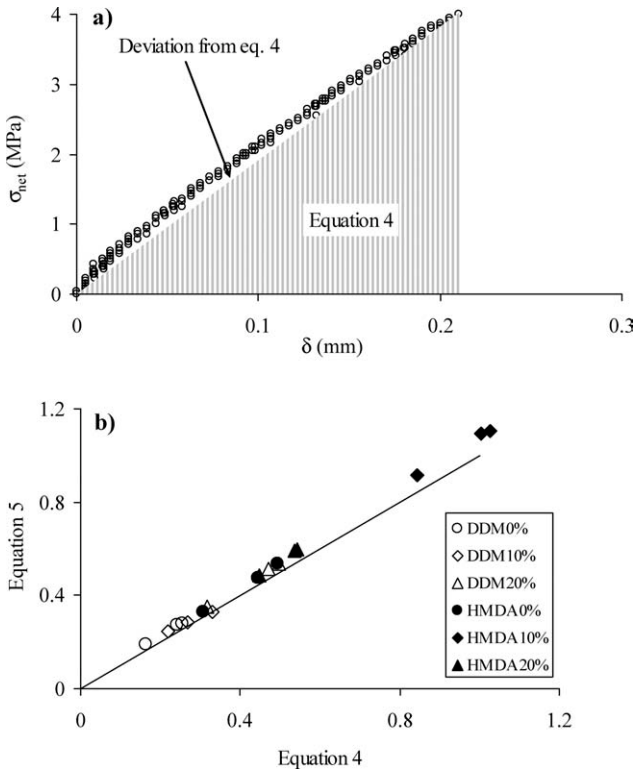

Figure 12 Fracture energy at initiation E_F: (a) Measurements of the area under the curve according to eqs. (4) and (5); (b) Deviation from linearity.

general concept of the J-integral[12] at crack initiation is utilized. This quantity is equivalent to the critical energy release rate when the material is linear elastic. Following[13] the area under the net stress versus δ curve is considered here as proportional to the toughness G_{IC}. Let E_F be this area representative of the fracture energy at crack initiation. When the material exhibits linear net stress versus δ curve, E_F can be expressed as:

$$E_F = \frac{1}{2}\sigma_{\text{net}}^{\max}\delta(\sigma_{\text{net}}^{\max}). \tag{4}$$

Accounting for the nonlinearity, E_F can be determined by a simple numerical integration:

$$E_F = \sum_{2}^{n_{\max}} \frac{\sigma_{\text{net}}^{n} + \sigma_{\text{net}}^{n-1}}{2}\left(\delta(\sigma_{\text{net}}^{n}) - \delta(\sigma_{\text{net}}^{n-1})\right), \tag{5}$$

where σ_{net}^{n} is the net stress at line n and $\delta(\sigma_{\text{net}}^{n})$ is the corresponding COD. Figure 12(a) shows the difference between eq. (4) and eq. (5) in the case of DDM0% curves.

E_F is expressed in kJ m^{-2}, when the net stress is in MPa and the δ in mm. This quantity has the same unit as the toughness in terms of G_{IC} (energy release rate). The main advantage of eq. (5) is that E_F can be directly accessed from experimental curve without any formula requirement. Nevertheless, the conclusions concerning E_F can be completely transferred to toughness.

To check at what extent is the deviation from linearity, with the help of experimental data, eq. (5) was plotted versus eq. (4) in Figure 12(b). The solid line represents the locus of experimental points when they fully satisfy linear conditions. It can be observed that all points lay over this solid line. Deviation is very slight for low E_F and is moderately increasing at high E_F.

Figure 13 illustrates the evolution of E_F—so the toughness—for both DDM and HMDA materials according to the AP-additive contents. The same trend as in Figure 10(a) can be observed. This clearly indicates that the maximum net stress is the leading parameter for the toughness. Indeed, for the materials of interest, toughening (enlarging the area under net stress versus δ curve) is obtained due to increased value of the maximum net stress without any embrittlement effect. Increase of the maximum net stress is essentially due to the increase of Young's modulus. Therefore, all the above-mentioned comments about the maximum net stress [Fig. 10(a)] are valid here. In particular, the abnormal drop in toughness for HMDA20% can be considered as a salient point needing further discussion.

Figure 5 showed that adding 20 mol % of AP-additive on DDM material resulted in toughness (G_{IC}) improvement from 0.3 kJ m^{-2} to 1.2 kJ m^{-2} at 20°C. As illustrated in Figure 13, the new campaign of tests reproduces the same result. Indeed, open circles corresponding to DDM material show that increasing AP-additive from 0 to 20% leads to an increase in E_F from 0.2 kJ m^{-2} to 0.3 kJ m^{-2}. Note also that 10% AP-additive on DDM content is not so much effective in toughening effect, whereas on HMDA the optimum value of improvement seems to be obtained for 10% AP additive.

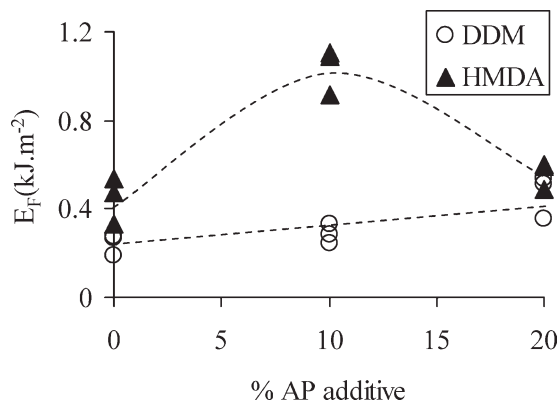

Figure 13 Fracture energy at crack initiation (toughness) plotted against AP-additive content for DDM and HMDA materials. Dashed lines were drawn to highlight the observed trends.

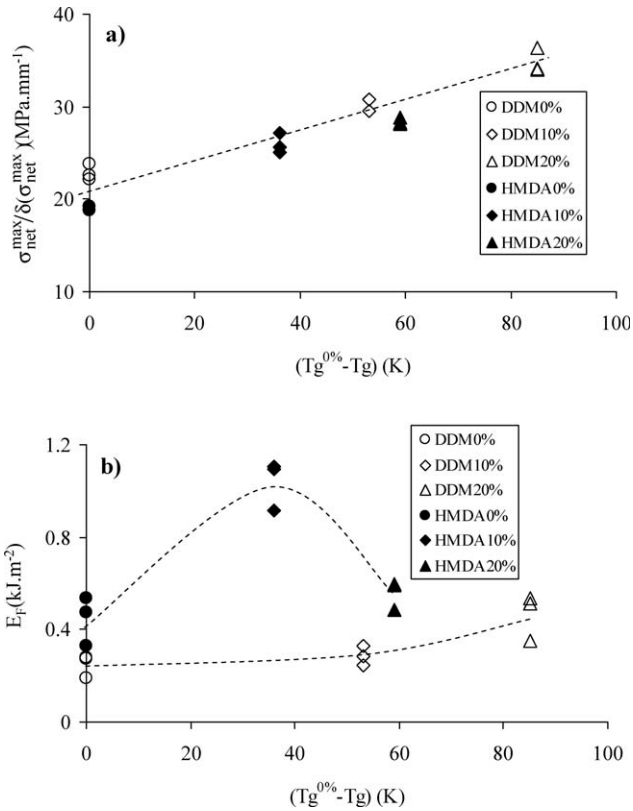

Figure 14 Correlation with respect to ($T_g^{0\%} - T_g$) for DDM and HMDA materials: (a) Stiffness (Young's modulus); (b) fracture energy at crack initiation (toughness). $T_g^{0\%}$ is the T_g of the unfilled material. Dashed lines were drawn to highlight the observed trends.

Energy fracture at crack initiation according to characteristic temperatures

In this section, discussion is focused on the parameter that is linked to the toughening effect. To do this, stiffness (Young's modulus) and E_F (toughness) curves were selected. The AP-additive contents were used to comment on the effect of all mechanical parameters before. Table II showed that the variation of AP-additive content induced also change in T_g measured via DSC technique. Furthermore, HMDA was primarily selected in this study to get a shift in T_g, from that of DDM. An attempt is made here, to use two characteristic temperatures:

- $T_g^{0\%} - T_g$ is the measure of each material change in T_g due to change in AP-additive content. The reference transition temperature $T_g^{0\%}$ is the one of the unfilled resin, say 180°C for DDM and 114°C for HMDA.
- $T_{test} - T_g$ is the gap between T_g and the test temperature (named T_{test}). In the conditions under consideration here, $T_{test} = 20$°C.

Note that the present tests being quasi-static, self heating is no accounted for here. Furthermore, the present tests were carried out at fixed T_{test} of 20°C and T_g changes according to the material tested, whereas for tests of Figure 5, both temperatures change: T_{test} ranges from −25 to 85°C and T_g of DDM 0% and DDM20% also varies.

Correlation with $T_g^{0\%} - T_g$

Figure 14(a) relates the stiffness to ($T_g^{0\%} - Tg$). The evolution of all experimental points is linear. Apart from the slight shift between the stiffness of unfilled DDM0% and HMDA0%, good agreement is obtained in the correlation. This seems to indicate that the evolution of the Young's modulus is controlled by the T_g shift due to the addition of the AP-antiplasticizer. This is partially highlighted by the shape of DMA traces in Figure 3(a). T_g is decreased from 180°C for DDM0% to 114°C for DDM20% but the appearance of μ-phase changes the shape of the storage modulus evolution. In particular, at room temperature (20°C), the Young's modulus of the DDM20% is higher. This can be extended to temperatures ranging between the two points where both curves intersect. In the case of Figure 3(a) for DDM material these temperatures are within the interval

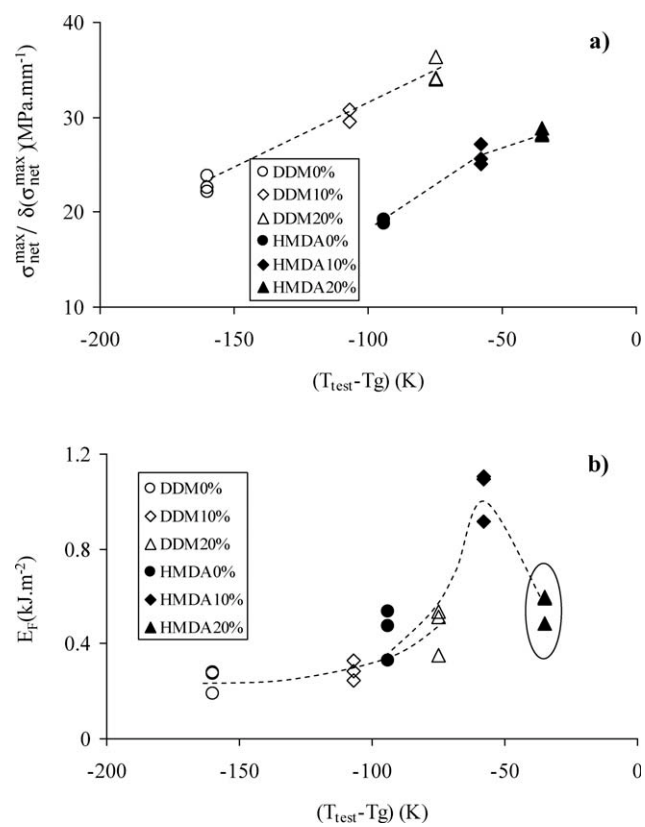

Figure 15 Fracture energy at crack initiation according to characteristic temperatures for DDM and HMDA materials (a) against deviation from T_g of materials without additive (b) against deviation between T_g and the test temperature. Dashed lines were drawn to highlight the observed trends.

−50°C and 80°C. Inspection of Figure 14(a) seems to indicate that this phenomenon can be continuously obtained for AP-additive contents ranging from 0 to 20%, equivalently for ($T_g^{0\%} - T_g$) ranging from 0 to 90°C. It can be mentioned that at least for both materials and within the investigated ranges, an equivalence between % AP-additive and ($T_g^{0\%} - T_g$) was obtained here. Figure 14(b) shows the correlation between E_F and ($T_g^{0\%} - T_g$). This operation seems not to "unify" the experimental points. Indeed, the same shape as in Figure 13 is obtained whatever the abscissa. In conclusion, increasing the AP-additive contents (from 0 to 20%) results in a decrease in T_g accompanied by a change of shape of the DMA curve that, in turn, allows an increase of the Young's modulus in a range of temperatures.

Correlation with $T_{\text{test}} - T_g$

The same approach as in previous subsection is applied here. First, the stiffness is plotted against ($T_{\text{test}} - T_g$) in Figure 15(a). No correlation seems to appear. In particular, the graph clearly indicates that the use of this ($T_{\text{test}} - T_g$) variable may hide the stiffening effect on HMDA0% compared with DDM0%. To go further, E_F is plotted as a function of ($T_{\text{test}} - T_g$) in Figure 15(b). An interesting effect is that HMDA0% and DDM20% approximately exhibit the same E_F for the same ($T_{\text{test}} - T_g$). An equivalence (% AP-additive) versus ($T_{\text{test}} - T_g$) is established for both materials and limited by at ($T_{\text{test}} - T_g$) < −50°C, in terms of toughness. Optimum toughening seems to be reached by cumulating the effect of T_g (DDM0% → HMDA0%) and that of (10% AP-additive) on HMDA material. This conclusion offers the possibility to improve toughening either by selecting one hardener and adding antiplasticizer with optimal content, or by choosing other hardener that make an equivalent shift on T_g. According to Figure 15(a), this latter case may suffer from a decrease in the Young's modulus.

The last issue to be discussed is the origin of the embrittlement observed in the HMDA series for an AP additive content of 20 mol % [Figs. 14(b) and 15(b)] This peculiar feature, already anticipated from the examination of the fracture surface [Fig. 9(c)], can be explained by recalling that T_g of the α phase is quite low in that case and falls in the temperature range where T_μ is likely to happen. Thus, from a molecular point of view, there is no significant contrast in segmental mobility within the two phases α and μ, a condition which is probably a prerequisite for toughening. On the other hand, lack of mobility contrast between the phases is not likely to affect the antiplasticization at lower temperature, as corroborated by the expected value of stiffness [Figs. 14(a) and 15(a)].

CONCLUSIONS

This study on the toughening of epoxy resins by phase separating antiplasticizers is based on a more refined mechanical analysis than the usual G_{Ic} measurements performed earlier.[6]

First, it fully confirms the suitability of the toughening strategy under study.

Second, it highlights some key factors for toughening, including:

- the gap between the T_g of the modified resins and of the neat resin
- the gap between the T_g of the α phase and the test temperature
- the gap between T_α and T_μ, the glass transition temperatures of the α and μ phases.

Finally, thanks to the examination of model systems, the study discusses the optimal conditions of toughening using the nanophase separation method and is, therefore, of interest for forthcoming upgraded formulations.

The authors would like to acknowledge Julie Heurtel (Mines ParisTech) and Freddy Martin (ESPCI ParisTech) for technical support.

References

1. Folch, L.; Burdekin, F. Eng Fract Mech 1999, 63, 57.
2. Rossol, A.; Berdin, C.; Prioul, C. Int J Fract 2002, 115, 205.
3. Tanguy, B.; Bouchet, C.; Bugat, S.; Besson, J. Eng Fract Mech 2006, 73, 191.
4. Corté, L.; Leibler, L. Macromol 2006, 39, 9365.
5. Halary JL.; Lauprêtre, F.; Monnerie, L. Polymer Materials: Macroscopic Properties and Molecular Interpretations. Wiley, Hoboken (NJ), 2011, ch. 13.
6. Sauvant, V.; Halary, J. L. J Appl Polym Sci 2001, 82, 759.
7. Martin, F.; Halary, J. L. Proceedings of 14th International Conference on Deformation, Yield and Fracture of Polymers (DYFP 2009), Kerkrade, Netherlands, 5–9 April 2009. p 149.
8. Halary, J. L.; Lauprêtre, F.; Monnerie, L. In Intrinsic Molecular Mobility and Toughness of Polymers (I); Kausch, H. H., Ed.; Adv Polym Sci 2005, 189, 35–213.
9. Kiefer, J.; Kausch, H. H.; Hilborn, J. G. Polym Bull 1997, 38, 477.
10. Sauvant, V.; Lauprêtre, F. Polymer 2002, 43, 1259.
11. Tada, H.; Paris, P. C.; Irwin, G. R. The Stress Analysis of Cracks Handbook. American Society of Mechanical Engineers, 3rd ed.; Wiley VCH, New York, 2000.
12. Rice, J. R. J Appl Mech 1968, 35, 379.
13. Landes, J. D.; Begley, J. A. Fracture Analysis, STP 560. American Society for Testing Analysis: Philadelphia, 1974, 170.